

Part of Special Issue
Phase-change memory: Science and applications

Midgap states, Raman scattering, glass homogeneity, percolative rigidity and stress transitions in chalcogenides

P. Boolchand*, K. Gunasekera, and S. Bhosle

School of Electronics and computing Systems, College of Engineering and Applied Science, University of Cincinnati, Cincinnati, OH 45221-0030, USA

Received 14 June 2012, revised 5 August 2012, accepted 6 August 2012

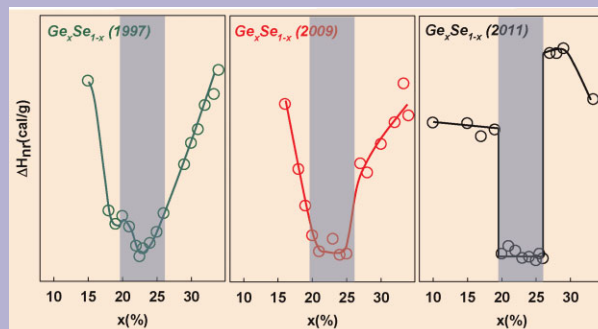
Published online 13 September 2012

Dedicated to Stanford R. Ovshinsky on the occasion of his 90th birthday

Keywords intermediate phase, midgap states, Raman scattering, rigidity theory

* Corresponding author: e-mail boolchp@ucmail.edu, Phone: +1-513-556-4758, Fax: +1-513-556-4790

Raman scattering from binary $\text{Ge}_x\text{Se}_{100-x}$ glasses excited using 1064 nm radiation display vibrational modes whose linewidths significantly exceed those observed using 647 nm radiation. In these glasses, 1064 nm radiation excites midgap states while 647 nm radiation excites conduction band tail states. Presence of midgap states in glasses, ascribed to coordination defects, is responsible for vibrational mode broadening that smears glass compositional variation of mode frequency using 1064 nm radiation but not with the 647 nm radiation. In the latter, mode-frequency variation of Corner-Shared (CS) and Edge-sharing (ES) tetrahedral units, in specially prepared homogeneous glasses, display thresholds near the rigidity ($x = 19.5\%$) and stress ($x = 26.0\%$) transitions, opening an intermediate phase (IP) that correlates well with the reversibility window (blue region) observed in calorimetric measurements (figure on the right).



Compositional trends in the non-reversing enthalpy of relaxation at T_g , $\Delta H_{nr}(x)$, in binary $\text{Ge}_x\text{Se}_{100-x}$ glasses examined in 1997, 2009, and 2011. The reversibility window (blue region) progressively sharpens to acquire a square-well like behaviour as melts/glasses homogenize. Figure taken from Ref. [1].

© 2012 WILEY-VCH Verlag GmbH & Co. KGaA, Weinheim

1 Introduction Stan Ovshinsky is widely recognized [2] for the phenomenon of electrical switching in amorphous Telluride films, which is the basis of rewritable phase change memories [3] today. The late David Adler in 1982 provided a historical perspective on the contributions of Stan Ovshinsky that anyone interested in science and technology of amorphous semiconductors would not want to miss reading [4]. Memories based on conducting bridge RAM using amorphous chalcogenide films are now being developed [5]. One of us (PB) had the great privilege to meet Stan Ovshinsky and work with his close associate, John deNeufville in 1971 at energy conversion devices (ECD).

The interaction with ECD stimulated our entry in the field of glass science. Bernard Goodman with his very diverse interests in condensed matter theory, has been a particular resource to PB in clarifying theoretical concepts in crystalline and glassy solids, including entropy considerations in the intermediate phase (IP). Over the years, Stan Ovshinsky and Bernie Goodman both have played an important role on glass science, and it is a pleasure to dedicate this article to them.

Rigidity theory [6, 7] has opened new vistas in understanding the disordered state of matter since its introduction in the early 1980s. Nearest-neighbour bond-stretching

and next-nearest-neighbour bond-bending interactions in covalent networks act as mechanical constraints, and have led to specific local structures (tetrahedra, pyramids) forming in glasses as melts are cooled past T_g . Enumeration of these constraints per atom (n_c) has proved to be remarkably useful in predicting elastic response of glassy networks. 3D Networks with $n_c < 3$ are, in general, characterized by floppy modes [8] ($f = 3 - n_c$) and are elastically flexible. Here, f represents the count of floppy modes per atom. Rigidity theory predicted [6] flexible networks would spontaneously become stressed-rigid as $n_c > 3$, or as their mean coordination number, $\bar{r} > 2.40$. At $\bar{r} = 2.40$, glassy networks are isostatic and that condition is widely identified with optimization of the glass forming tendency. However, experiments on real glasses in the laboratory reveal that onset of rigidity and stress do not occur at the same network connectivity as was predicted by theory, but it generally occurs at two distinct values of \bar{r} , with rigidity percolating first ($\bar{r}_c(1)$) as the floppy mode count vanishes within Maxwell counting, followed by percolation of stress at a slightly higher connectivity ($\bar{r}_c(2)$) as redundant bonds first manifest in networks. The most unusual physical properties of glassy networks formed between these two transitions, $\bar{r}_c(2) < \bar{r} < \bar{r}_c(1)$, led to the discovery [9, 10] of the IP, and the notion of self-organization. [11] Glassy networks when optimally constrained ($n_c = 3$), experiments show, acquire a new functionality to adapt [12] and reconnect, expel stress, display thermally reversing glass transitions, fill space efficiently and show little or no aging. These physical properties were not a part of our experience earlier in the field. More recently, *ab initio* MD simulations [13] have opened a new direction to quantitatively identify mechanical constraints in glassy networks that are intact from those that are broken by establishing standard deviations of bond-lengths and bond-angles. These MD simulations reveal, *e.g.*, justification for the 8-N bonding rule in sulphide and selenide glasses [13]. These new developments have also permitted to extend the original $T = 0$ K, rigidity theory to finite temperatures [14, 15] and to modified oxides [16], and to networks containing tellurium as in the case of the phase change materials (Ge–Sb–Te) in which the 8-N bonding rule is broken. Rigidity theory has made feasible constructing elastic phase diagrams [17] in several families of oxides and chalcogenides opening a novel means to characterize glass functionality.

2 Slow homogenization of glassy melts Since elastic phase transitions in glassy networks are usually inferred from compositional studies of their thermal, optical, mechanical and electrical behaviour, the need of *dry* and *homogeneous* glass compositions at non-stoichiometric chemical compositions is paramount not only to probe basic science but also to optimize glass properties in commercial applications. Recently we introduced an FT-Raman profiling method to monitor growth of homogeneity of chalcogenide melts in punctuated off line experiments, and showed that these undergo slow homogenization. The idea was demon-

strated [1, 18, 19] for the case of the well-studied [20] $\text{Ge}_x\text{Se}_{100-x}$ binary glass system, wherein 2 g sized melts were synthesized by reacting 99.999% pure Ge and Se pieces (3–4 mm) in evacuated (1×10^{-7} Torr) quartz tubes (5 mm id) at 950 °C for various times, t_R , extending up to 192 h. For the case of a GeSe_2 melt (Fig. 1), FT-Raman spectra were acquired at 9 equally spaced locations along the length of a one inch long quenched-melt in a quartz tube. These results as a function of increasing t_R show that the 9 spectra became identical after 192 h of reaction time, showing that the batch composition had globally homogenized. Following this procedure, we synthesized 20 other glass compositions

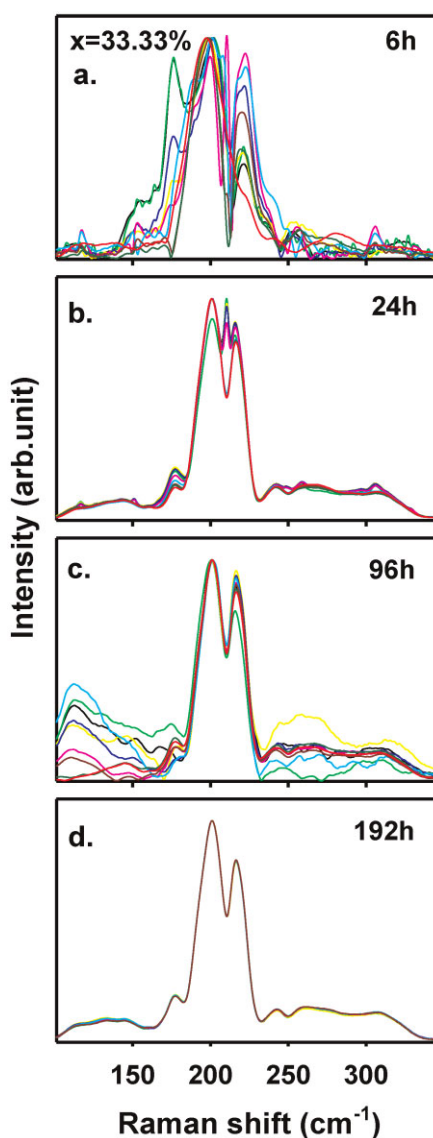


Figure 1 (online colour at: www.pss-b.com) FT-Raman profiling results on a GeSe_2 melt after the starting materials (Ge, Se) were reacted for (a) 6 h, (b) 24 h, (c) 96 h and (d) 192 h. Note that the 9 Raman lines shape taken along length of the quenched melt become identical after 192 h, showing that the 2 g batch has homogenized on a scale of 10 μm . Figure taken from Ref. [19].

in the Ge–Se binary, and comprehensively examined their physical properties [1, 18, 19]. In such glass samples of proven homogeneity, the non-reversing enthalpy of relaxation at T_g , $\Delta H_{nr}(x)$, shows a square-well like thermally reversing window (figure next to abstract) with abrupt walls. These walls near $x = 19.5$ and 26% represent the onset of percolative rigidity and stress transitions, respectively. The near vanishing of $\Delta H_{nr}(x)$ term in the IP is due to the isostatic character of glass compositions in that phase [21]. The reversibility window in Ge–Se glasses underwent a change from being triangular in 1997, to becoming trapezoidal in 2009, and to finally acquiring a square-well like behaviour in 2011 as melts became steadily more homogeneous. In these three sets of measurements carried out at University of Cincinnati over the past 13 years the only variable in homogenization of melts was the reaction time, t_R , of the starting materials at 950 °C; it was 48 h in 1997, 96 h in 2009 and 192 h in 2011. These new developments have finally addressed a crucial experimental issue in the field-synthesis of homogeneous non-stoichiometric glass compositions, a prerequisite to addressing the physics of network glasses and melts.

Reversibility windows have also been reported in other selenides, sulfides [22, 23], tellurides [24, 25], modified oxides [26, 27] and Ag-based solid electrolytes [28]. The group at the Indian Institute of Science, Bangalore, has reported observation of such windows in several families of phase-change materials [24, 29].

3 Variation of Raman vibrational mode-frequency and mode-widths in Ge–Se glasses

Figure 2 gives a summary of the compositional variation of mode frequency of the Corner-Sharing (CS) and Edge-Sharing (ES) tetrahedra, $\nu_{CS}(x)$, $\nu_{ES}(x)$, in binary Ge–Se glasses examined in FT-Raman and dispersive Raman scattering experiments [18, 19]. One finds both $\nu_{CS}(x)$, $\nu_{ES}(x)$, vary smoothly and continuously with x in FT-Raman experiments. On the other hand, the variation of $\nu_{CS}(x)$, $\nu_{ES}(x)$, in the dispersive Raman experiments show thresholds near $x_c(1) = 19.5\%$, $x_c(2) = 26.0\%$ and $x_c(3) = 31.5\%$. These thresholds represent onset of rigidity, stress and nanoscale phase separation (NSPS), respectively [1]. Why such a wide difference in the variation of $\nu_{CS}(x)$, $\nu_{ES}(x)$ between the two types of Raman scattering experiments on the same samples?

Experimentally, the clue resides in the linewidth, full-width at half maximum, $\Gamma(x)$ variation of the vibrational modes. Raman lineshapes on these homogeneous samples were analysed as a superposition of Gaussians keeping mode-centroid, -intensity and -linewidths as variables in the non-linear least squares fit. The results for the CS mode linewidth appear in Fig. 3. One finds that although $\Gamma(x)$ increases steadily with x in both types of Raman measurements, the observed linewidths in the FT-Raman measurements are consistently 15–30% wider than those in dispersive ones. As a consequence of the broad linewidths, elastic thresholds tracked by the variation in mode

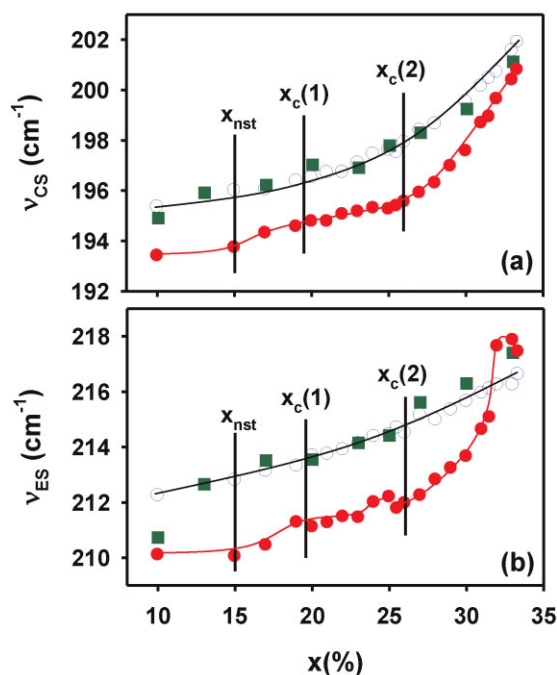


Figure 2 (online colour at: www.pss-b.com) (a) Observed CS and (b) ES Raman mode frequency variation in $\text{Ge}_x\text{Se}_{100-x}$ glasses in FT-Raman (○) and dispersive Raman (●) scattering experiments. The (■) data points are taken from Ref. [30] of Gjersing et al. and represent FT Raman results on $\text{Ge}_x\text{Se}_{100-x}$ glasses. x_{nst} marks the onset of non-stochastic structure Ref. [1]. Error in open and filled circle data points is equal to the size of the data points.

frequency, $\nu_{CS}(x)$ and $\nu_{ES}(x)$ are washed out in the FT-Raman experiments. Our results for $\nu_{CS}(x)$ and $\nu_{ES}(x)$ in the FT-Raman measurements are quite similar to those reported recently by Gjersing et al. [30]. These results, as we show next, not only provide experimental evidence for the existence of midgap states in chalcogenides glasses but also serve to illustrate that Raman scattering can be selectively used to probe either the defected or the normal

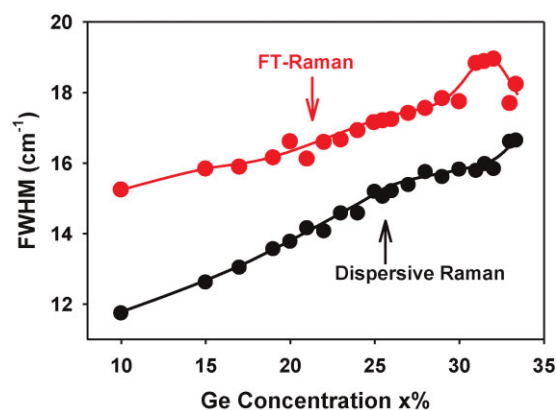


Figure 3 (online colour at: www.pss-b.com) Observed FWHM of CS mode in FT- and dispersive-Raman scattering of $\text{Ge}_x\text{Se}_{100-x}$ glasses.

part of a network by merely tuning the exciting radiation in the optical gap of these materials.

There are two features of interest in the $I(x)$ plots of Fig. 3. One is that in both types of Raman scattering experiments $I(x)$ increases by about 4 cm^{-1} across the range of compositions examined; the increase is from 12 to 16 cm^{-1} in the dispersive, and from about $15\text{--}19\text{ cm}^{-1}$ in the FT-Raman experiments. Second, $I(x)$ in the FT-measurements are consistently higher than those in dispersive measurements anywhere from 30% at $x=10$ to 15% at $x=33.3\%$. The first feature is intrinsically tied to the deformation of GeSe_4 tetrahedra as the topology of the glassy networks undergoes a change from being flexible at low x ($<19.5\%$) to stressed-rigid at high x ($>26\%$). Recently Bauchy et al. [13] have shown from MD simulations that the standard deviation ($\sigma(x)$) of the Ge tetrahedral bond angle increases from 8 degrees at $x=10\%$ to an average of about 14 degrees at $x=33.3\%$, while the Se bond angle remains largely well defined across the wide range of x . The GeSe_4 tetrahedra clearly distort as flexible glasses become stressed rigid. The second issue is that the photon energy used in the FT-Raman experiments selectively excites midgap electronic states while that used in dispersive Raman measurements excites conduction band tail states. That circumstance has the consequence of broadening the vibrational density of states of glasses in the former, and we comment on the issue next.

4 Midgap states, optical bandgaps and Raman scattering

For several decades the existence of midgap states in glassy and amorphous semiconductors has been recognized from Stokes shift of photoluminescence (PL) [31, 32]. Ball et al. [31], *e.g.*, have reported the PL peak in binary Ge–Se glasses to shift to the middle of the gap, $E_g/2$, where E_g represents the gap at $\alpha = 1 \times 10^3\text{ cm}^{-1}$. The origin of these electronic states deep in the gap have been identified with coordination defects such as valence alternation pairs [33, 34] and homopolar bonds. Compositional trends in optical bandgap of binary Ge–Se thin-films have been measured by several groups [35–38], and as the quality (stoichiometry and disorder) of deposited films have improved, optical gaps have steadily increased.

In the experiments of Jin et al. [36] the evaporation charge used to deposit a thin-film was the corresponding bulk glass. Raman scattering of bulk glasses were recorded, and compared to those of evaporated thin-films. In each case, the similarity of Raman scattering confirmed that the stoichiometry of the evaporated thin-films was close to that of corresponding bulk glasses. In these experiments evaporated films, typically about $1\text{ }\mu\text{m}$ in thickness, were relaxed at room temperature for two years prior to undertaking the optical absorption measurements. Figure 4 shows the compositional variation of the optical gap $E_{53}(x)$, corresponding to an absorption coefficient, $\alpha = 5 \times 10^3\text{ cm}^{-1}$, and of the Tauc edge, $E_T(x)$, obtained the usual way [36]. The optical gap, $E_{53}(x)$, is found to increase from about $2.18(3)\text{ eV}$ at $x=15\%$ to about $2.32(3)\text{ eV}$ at $x=33.3\%$.

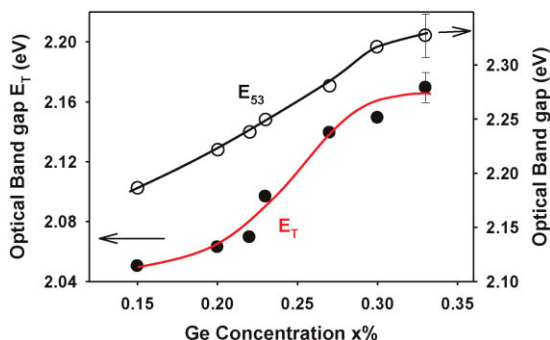


Figure 4 (online colour at: www.pss-b.com) Optical band gap, $E_{53}(x)$, corresponding to an optical absorption of 5×10^3 , and Tauc edge (E_T) of $\text{Ge}_x\text{Se}_{100-x}$ thin-films reported in Ref. [36]. Note that $E_T(x)$ for the films all exceed the 1.91 eV photon energy used in the dispersive measurements. Furthermore, the photon energy of 1.16 eV used to excite FT-Raman scattering in the Ge–Se glasses reside near the midgap value of 1.11 eV.

The Tauc edge, $E_T(x)$, also increases from $2.04(3)\text{ eV}$ at $x=15\%$ to $2.16(3)\text{ eV}$ at $x=33.3\%$. These results are similar to those reported by Sleenckx et al. [37] but less so to the earlier work in the field [35, 38]. The $E_{53}(x)$ results place the average midgap near 1.12 eV, close to the excitation energy (1.17 eV) used in the FT-Raman experiments. In the dispersive Raman experiments, the excitation energy of 1.91 eV, places it in the conduction band tails states below the Tauc edge of all glass compositions. These conditions underscore the fact that both Raman experiments essentially probe the bulk structure of Ge–Se glasses.

Use of the NIR radiation in the FT-Raman experiments, however, leads to selectively probing the defective part of the glass network while use of red light in the dispersive measurements to probing the normal part of the Ge–Se glass structure. For this reason, one can expect the linewidth of the CS mode in FT-Raman experiments to be greater than in the dispersive Raman ones. The data of Fig. 3 shows the linewidth ratio, $I_{\text{FT}}^{\text{CS}}/I_{\text{DI}}^{\text{CS}}(x)$, to be 1.30 at $x=10\%$ and to steadily decrease to 1.15 as x increases to 33.3%. The systematic reduction of the ratio, most likely, results because of the energy gap of the glasses increases with x . The FT-Raman radiation then excites states increasingly below the midgap region, in effect then probing less of the defective part of the network. These results are reminiscent of Raman scattering on diamond-like carbon films [39]; with visible radiation accessing sp^2 -like carbon of a graphitic origin, while with UV radiation probing sp^3 -like tetrahedral carbon in the films. These results point to the versatility of Raman scattering to select various parts of a network by tuning the excitation radiation. Noteworthy is the fact that near and in the defected regions network structure appears to have changed compared to the normal part of the network. One observes a blue-shift of about 2 cm^{-1} in both $\nu_{\text{CS}}(x)$ and $\nu_{\text{ES}}(x)$ across the range of x studied (Fig. 2) suggesting that the defective part is stiffer than the normal part of the

network. Small changes in long-range structure apparently must occur to produce large effect on the elastic response of these defected regions where self-organization effects appear to be suppressed.

5 Topology and nanostructure of binary Ge–Se glasses

The *structural* interpretation of the glass transition temperature, T_g , as a measure of network *connectivity* [40], and the Naumis interpretation of T_g a measure of network rigidity [41] lend well to understanding the molecular structure of present binary glasses. At low x (<15%), Ge *stochastically* cross-links polymeric Se_n -chains. In the Stochastic agglomeration theory, parameter free $dT_g(x)/dx$ slopes are predicted [40] in terms of coordination numbers of the base glass (Se, $r = 2$) and the additive (Ge, $r = 4$) that are found to be in excellent accord with experiments. As $x > 15\%$, a *non-stochastic* evolution of glass structure ensues; CS tetrahedral units grow superlinearly with x with little or no change in ES units in the $15\% < x < 20\%$ range (see Fig. 8 in Ref. [1]) as precursive to networks self-organizing as x increases to near 20%. The IP extends in the $19.5\% < x < 26\%$ range of Ge, and one finds the concentration of CS tetrahedral units appear to remain unchanged with x . Once the Ge content of glasses exceeds 26%, ES tetrahedral units grow precipitously in the stressed-rigid phase. Networks containing up a 31.5% of Ge are fully polymerized. However, once $x > 31.5\%$, some of the alloyed Ge nucleates a separate Ge-rich ethane like phase for which evidence is given by ^{119}Sn Mössbauer spectroscopy [42], Raman scattering [42], the non-reversing enthalpy of relaxation at T_g and the slope dT_g/dx , each of which reveal a threshold behaviour near this composition. The loss of network connectivity because of the onset of NSPS is reflected in both thermal and vibrational behaviour of glasses [1]. NSPS of stressed-rigid glasses is not peculiar to the present binary but is observed widely in other families of binary [23, 43] and ternary [44] chalcogenides. It provides a natural way in which stress or free energy of the fully polymerized network is lowered by segregating into two nanophases of lower connectivity.

One can schematically describe glass structure evolution in terms of topology with the aid of Fig. 5. With increasing Ge content, glasses transit from being flexible to becoming stressed-rigid but only after passing through an IP. The existence of this phase in real glasses is nature's way to expel stress and self-organize networks in a limited range of connectivity. Although this phase is relatively narrow in the present binary, there are sound reasons to believe that its width can be increased in multicomponent glasses [45]. This phase is not merely of basic interest but it is of direct relevance to applications of amorphous and glassy materials in emerging new technologies because of its intrinsically non-aging character. It is particularly opportune to emphasize the importance of this phase in this article dedicated to Stan Ovshinsky, who has always sought new and exciting opportunities of using amorphous materials to betterment of human life.

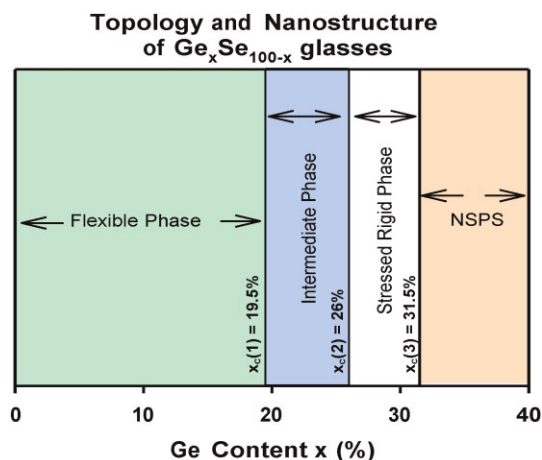


Figure 5 (online colour at: www.pss-b.com) Elastic phases of binary Ge–Se glasses in terms of their topology. NSPS, nanoscale phase separation. See text.

Evidence for flexible, intermediate and stressed-rigid elastic phases in bulk $Ge_xSi_xTe_{100-2x}$ glasses, a phase change material, has recently emerged [46] from calorimetric and molar volume measurements. As in the case of selenides, one finds that synthesis of dry and homogeneous bulk glasses is a prerequisite to observe clearly defined reversibility- and molar volume-windows in the $7.5\% < x < 9\%$ range. And as the content x of the group IV additives in Te increases, evidence of NSPS is observed as $x > 12\%$. Thus, topology plays the central role in defining the elastic phases in the Ge–Si–Te ternary, much like in the Ge–Se binary as we have seen above.

6 Conclusions As the quality of binary Ge_xSe_{100-x} glasses, particularly their dryness and homogeneity has improved, compositional variation of physical properties are found to display three threshold compositions; $x_c(1) = 19.5(3)\%$, $x_c(2) = 26.0(3)\%$ and $x_c(3) = 31.5(3)\%$. These threshold compositions are identified, respectively, with percolation of rigidity, percolation of stress and onset of chemical phase separation on a nanoscale. These thresholds are observed in thermal, optical and mechanical measurements. In these high quality glasses, midgap electronic states representing defect coordinations persist. Raman scattering using NIR radiation (1064 nm) can selectively excite midgap states and measurably broaden vibrational modes. On the other hand, visible Raman scattering using 647 nm radiation, excites states below the Tauc edge and probe normal part of a network.

Acknowledgements We acknowledge ongoing discussions with M. Micoulaut, J. C. Phillips, R. Zallen, J. Mauro, D. McDaniel, Sergey Mamedov and Len Thomas. And it is pleasure to dedicate this paper to both Stan Ovshinsky and Bernie Goodman for their continued encouragement on glass science projects over the years. This work is supported by NSF grant DMR 08-53957.

References

- [1] S. Bhosle, K. Gunasekera, P. Boolchand, and M. Micoulaut, *Int. J. Appl. Glass Sci.* **3**(3), 205–220 (2012).
- [2] S. R. Ovshinsky, *Phys. Rev. Lett.* **21**, 1450 (1968).
- [3] M. Wuttig and N. Yamada, *Nature Mater.* **6**, 824 (2007).
- [4] D. Adler, in: *Disordered Materials: Science and Technology, Selected Papers by S. R. Ovshinsky*, edited by D. Adler (Amorphous Institute Press, Bloomfield Hills, MI, 1982), Introduction, p. vii.
- [5] N. Derhacopian, S. C. Hollmer, N. Gilbert, and M. N. Kozicki, *Proc. IEEE* **98**, 283 (2010).
- [6] J. C. Phillips and M. F. Thorpe, *Solid State Commun.* **53**, 699 (1985).
- [7] J. C. Phillips, *J. Non-Cryst. Solids* **34**, 153 (1979).
- [8] M. F. Thorpe, *J. Non-Cryst. Solids* **57**, 355 (1983).
- [9] D. Selvanathan, W. J. Bresser, and P. Boolchand, *Phys. Rev. B* **61**, 15061 (2000).
- [10] P. Boolchand, G. Lucovsky, J. C. Phillips, and M. F. Thorpe, *Philos. Mag.* **85**, 3823 (2005).
- [11] M. F. Thorpe and M. V. Chubynsky, in: *Phase Transitions and Self-organization in Electronic and Molecular Networks*, edited by J. C. Phillips and F. Thrope, *Fundamental Materials Research* (Kluwer Academic, Plenum Publishers, New York, 2001), chap. 1, pp. 43–64.
- [12] J. Barre, A. R. Bishop, T. A. Lookman, and A. Saxena, *Phys. Rev. Lett.* **94**, 208701 (2005).
- [13] M. Bauchy, M. Micoulaut, M. Celino, S. Le Roux, M. Boero, and C. Massobrio, *Phys. Rev. B* **84**, 054201 (2011).
- [14] P. K. Gupta and J. C. Mauro, *J. Chem. Phys.* **130**, 094503 (2009).
- [15] M. Bauchy and M. Micoulaut, *J. Non-Cryst. Solids* **357**, 2530 (2011).
- [16] M. Bauchy, M. Micoulaut, and P. Boolchand, (submitted).
- [17] M. Micoulaut, C. Otjacques, J.-Y. Raty, and C. Bichara, *Phys. Rev. B* **81**, 1 (2010).
- [18] S. Bhosle, K. Gunasekera, P. Chen, P. Boolchand, M. Micoulaut, and C. Massabrio, *Solid State Commun.* **151**, 1851 (2011).
- [19] S. Bhosle, K. Gunasekera, P. Boolchand, and M. Micoulaut, *Int. J. Appl. Glass Sci.* **3**(3), 189–204 (2012).
- [20] Y. Wang, M. Nakamura, O. Matsuda, and K. Murase, *J. Non-Cryst. Solids* **266-269**, 872 (2000).
- [21] M. Micoulaut, *J. Phys.: Condens. Matter* **22**, 1 (2010).
- [22] U. Vempati and P. Boolchand, *J. Phys.: Condens. Matter* **16**, S5121 (2004).
- [23] P. Boolchand, P. Chen, and U. Vempati, *J. Non-Cryst. Solids* **355**, 1773 (2009).
- [24] M. Anbarasu, K. K. Singh, and S. Asokan, *Philos. Mag.* **88**, 599 (2008).
- [25] M. Anbarasu, K. K. Singh, and S. Asokan, *J. Non-Cryst. Solids* **354**, 3369 (2008).
- [26] K. Rompicharla, D. I. Novita, P. Chen, P. Boolchand, M. Micoulaut, and W. Huff, *J. Phys.: Condens. Matter* **20**, 202101 (2008).
- [27] Y. Vaills, T. Qu, M. Micoulaut, F. Chaimbault, and P. Boolchand, *J. Phys.: Condens. Matter* **17**, 4889 (2005).
- [28] D. I. Novita and P. Boolchand, *Phys. Rev. B* **76**, 184205 (2007).
- [29] B. J. Madhu, H. S. Jayanna, and S. Asokan, *Eur. Phys. J. B, Condens. Matter Complex Syst.* **71**, 21 (2009).
- [30] E. L. Gjersing, S. Sen, and B. G. Aitken, *J. Phys. Chem. C* **114**, 8601 (2010).
- [31] G. J. Ball, J. M. Chamberlain, and T. Instone, *Solid State Commun.* **27**, 71 (1978).
- [32] H. Fritzsche, *Annu. Rev. Mater. Sci.* **2**, 697 (1972).
- [33] M. Abkowitz, *J. Chem. Phys.* **46**, 4537 (1967).
- [34] M. Kastner, D. Adler, and H. Fritzsche, *Phys. Rev. Lett.* **37**, 1504 (1976).
- [35] R. A. Street, R. J. Nemanich, and G. A. N. Connell, *Phys. Rev. B* **18**, 6915 (1978).
- [36] M. Jin, P. Chen, P. Boolchand, T. Rajagopalan, K. L. Chopra, K. Starbova, and N. Starbov, *Phys. Rev. B* **78**, 214201 (2008).
- [37] E. Sleetckx, L. Tich, P. Nagels, and R. Callaerts, *J. Non-Cryst. Solids* **198-200**, Part 2 723 (1996).
- [38] C. A. Spence and S. R. Elliott, *Phys. Rev. B* **39**, 5452 (1989).
- [39] Z. Sun, J. R. Shi, B. K. Tay, and S. P. Lau, *Diamond Relat. Mater.* **9**, 1979 (2000).
- [40] M. Micoulaut, *Eur. Phys. J. B* **1**, 277 (1998).
- [41] G. G. Naumis, *Phys. Rev. B* **73**, 172202 (2006).
- [42] P. Boolchand and W. J. Bresser, *Philos. Mag. B* **80**, 1757 (2000).
- [43] D. G. Georgiev, P. Boolchand, and M. Micoulaut, *Phys. Rev. B* **62**, R9228 (2000).
- [44] S. Mamedov, D. G. Georgiev, T. Qu, and P. Boolchand, *J. Phys.: Condens. Matter* **15**, S2397 (2003).
- [45] P. Boolchand, P. Chen, D. I. Novita, and B. Goodman, in: *Rigidity and Boolchand Intermediate Phases in Nanomaterials*, edited by M. Micoulaut and M. Popescu, *Optoelectronic Materials and Devices*, Vol. 6 (INOE, Bucharest, 2009), chap. 1, pp. 1–36.
- [46] K. Gunasekera, P. Boolchand, and S. Mamedov, *Proceedings American Phys. Soc. March Meeting, Boston, USA* (American Phys. Soc., College Park, 2012), <http://meetings.aps.org/link/BAPS.2012.MAR.Y7.8>.